Progress In Electromagnetics Research M, Vol. 84, 117–126, 2019

Dual Circularly Polarized Substrate Integrated Waveguide Cavity-Backed Antenna with Enhanced Bandwidth and Reduced Size for Wideband Wireless Applications

Tian Li*

Abstract—A dual circularly polarized (CP) substrate integrated waveguide (SIW) cavity-backed antenna with the feasibility of obtaining a wider bandwidth and relatively smaller size than other homogeneous referenced antennas is proposed and demonstrated. Fed by a quadrature hybrid coupler, the proposed double-layered stacked antenna, consisting of a perturbed circular SIW cavity and an improved circular patch radiator, is designed, analyzed, and fabricated. Good agreement between simulated and measured results is observed. Simulation and measurement results reveal that the proposed antenna can provide impedance bandwidths of 45.7% (4.74–7.55 GHz) and 46.2% (4.75–7.6 GHz), as well as 3-dB axial ratio (AR) bandwidths of 37.5% (4.74–6.93 GHz) and 37.2% (4.75–6.92 GHz) for RHCP and LHCP, respectively. Meanwhile, within the effective RHCP/LHCP bandwidths, the proposed antenna has gains from 4.8 dBic to 7.6 dBic with an average gain of 6.4 dBic for RHCP, and gains from 4.9 dBic to 7.5 dBic with an average gain of 6.3 dBic for LHCP, respectively. Additionally, the measured effective dual CP bandwidth of 37.2% (4.75–6.92 GHz) not only meets the need for certain Wi-Fi (5.2/5.8 GHz) or WiMAX (5.5 GHz) band communication application, but also provides the potential to implement multiservice transmission.

1. INTRODUCTION

Unidirectional dual circularly polarized (CP) antennas have attracted great attention due to their merits of capabilities of reducing polarization mismatch, suppressing multipath interference, realizing unidirectional radiation with higher gain, increasing the channel capacity and link robustness, and enhancing frequency reuse [1–11]. Meanwhile, dual CP substrate integrated waveguide (SIW) cavity-backed antennas have the inherent advantage of mitigating the effect of unexpected electromagnetic interference in the installment environment due to their self-consistent electrical shielding. Though the feature of broad 3 dB axial ratio (AR) bandwidth is becoming increasingly necessary due to the high data rate required by modern services, many newly published unidirectional dual-CP antennas in [4–10] only support relatively narrow-band applications. In [4], a dual CP SIW antenna consisting of a quarter-mode SIW cavity, two open stubs, and defected ground structures is presented, and it obtains an effective dual CP bandwidth of 11.2% and a much lower profile of $0.03\lambda_0$. In [5], a dual CP metasurface antenna (MSA) with large beamwidth is proposed, which obtains an effective dual CP bandwidth of 12.4%. In [6], a dual CP planar four-port aperture antenna with an effective dual CP bandwidth of 17.2% for 60 GHz applications is introduced. Moreover, a dual CP SIW cavity-backed patch antenna using a two-layer structure is presented in [7], while it has a limited effective dual CP bandwidth of 3.4%. In [8], a dual CP microstrip antenna is proposed, and it obtains a wider effective dual CP bandwidth of 19.4% by employing a novel vertically coupled resonator-based structure and the

Received 21 June 2019, Accepted 9 August 2019, Scheduled 26 August 2019
* Corresponding author: Tian Li (tianli@stu.xidian.edu.cn).
The authors are with the Southwest China Institute of Electronic Technology, Chengdu 610036, China.

intrinsic 90° phase difference between two coupling paths. Furthermore, in [9], a dual CP horn antenna based on multilayer SIW is reported, and it has an effective dual CP bandwidth of 11.8%. In [10], a dual CP antenna consisting of stacked square patches fed by striplines and a branch line coupler is presented, and it has an effective dual CP bandwidth of 13.0%. In addition, for a conventional cavity-backed antenna, the height of the metallic cavity is inclined to be approximately a quarter-wavelength to support its radiation modes. As presented in [11], the proposed conventional cavity-backed antenna obtains a wide effective RHCP bandwidth of 43.3%, whereas it does not provide dual-CP radiation, and its profile of 15 mm ($0.3\lambda_0$) is very high.

In this letter, a dual circularly polarized SIW cavity-backed antenna with an effective dual CP bandwidth of 37.2% and relatively low profile of $0.097\lambda_0$ is presented. Fed by a conventional quadrature hybrid coupler (Q-hybrid), the proposed double-layered stacked antenna is based on a perturbed circular SIW cavity and an improved circular patch. By loading two ring slots around the circular patch radiator's two feeding points, the antenna AR performance can be greatly enhanced, especially for lower frequencies. Meanwhile, four rectangular slots are symmetrically loaded on the circular patch radiator, which facilitates the shift of antenna operating band towards the lower band, thus contributing to a relatively compact size. Furthermore, a parasitic ring slot is etched on the upper metal layer of the SIW cavity to further improve the AR performance. For demonstration, the proposed antenna is fabricated and measured. The measured results have a reasonable agreement with the simulated ones.

2. ANTENNA CONFIGURATION

Figure 1 shows the geometry of the proposed double-layered stacked dual circularly polarized SIW cavity-backed antenna. The upper square substrate for the circular radiator and SIW cavity is with relative dielectric constant of 2.65, loss tangent of 0.0015, and size of 55.5 mm × 55.5 mm × 4 mm. The lower square substrate for the quadrature (90°) hybrid coupler consists of two substrates which are bonded together by the prepreg. The two substrates are with relative dielectric constant of 2.94 and loss tangent of 0.0012. The prepreg layer is with relative dielectric constant of 2.74 and loss tangent of 0.014. The total thickness of the Q-hybrid substrate is about 1 mm. A circular cavity with radius of 26.65 mm is produced by an annular array composed of 45 metallic vias with diameters of 1.2 mm and distances of 3.72 mm penetrating through the substrate of the radiator. Then a circular slot with radius of 17.5 mm is etched on the upper metal layer of the SIW cavity for the circular patch. The circular radiator is double-fed by the quadrature hybrid coupler with width of 7.7 mm, and they are connected

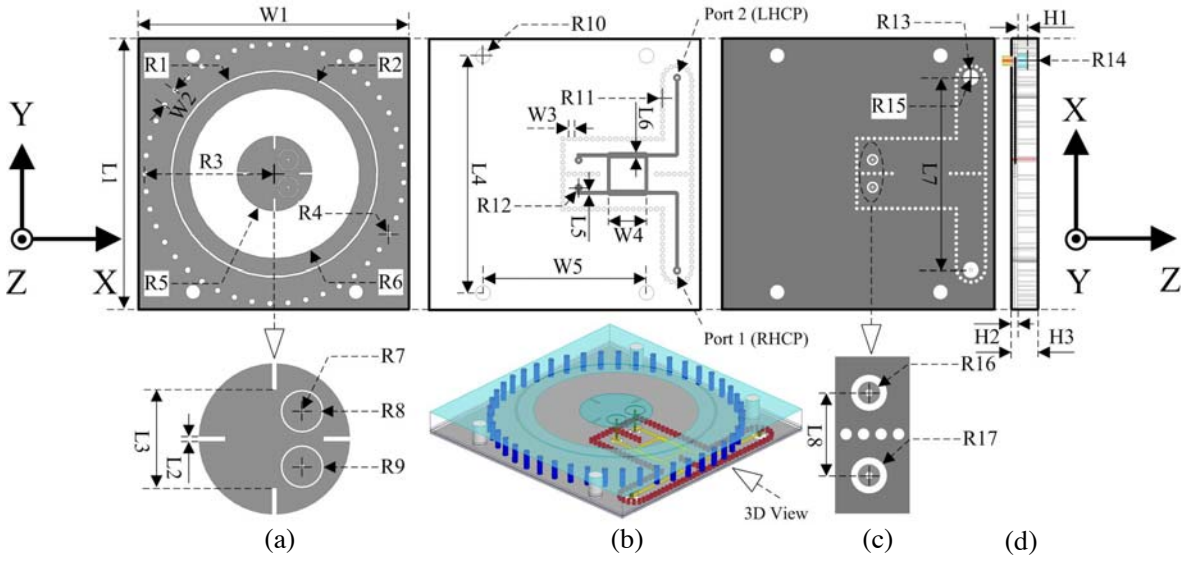

Figure 1. Configuration of the proposed antenna. (a) Front view; (b) Front view of the Q-hybrid's middle layer and 3D view of the proposed antenna; (c) Back view; (d) Side view.

by two metallic vias with diameters of 0.5 mm. To enhance the AR bandwidth, two ring slots with widths of 0.2 mm are loaded around the circular patch radiator's two feeding points. Meanwhile, four identical rectangular slots with widths of 0.5 mm are symmetrically loaded on the circular patch radiator, which facilitates the proposed antenna's miniaturization. Moreover, a parasitic ring slot with width of 0.5 mm is etched on the upper metal layer of the SIW cavity to further improve the AR performance. Furthermore, since the two SMA connectors are soldered from the back side of the proposed antenna, two blind vias with size of Φ 3 mm $\times$ 2 mm is designed in the upper substrate above the two feeding points of the quadrature hybrid coupler for solder joint avoidance. Finally, a set of air vias with radii of 1.5 mm are symmetrically loaded on the proposed double-layered stacked antenna acting as locating structures, which facilitate the proposed antenna's installation and welding. Detailed geometry and dimensions of the proposed antenna are given in Figure 1 and Table 1 after optimization using ANSYS HFSS.

Table 1. Dimensions of the proposed antenna (Unit: mm).

Parameter	Value	Parameter	Value	Parameter	Value
$L1$	55.5	$W4$	7.7	$R10$	1.5
$L2$	0.5	$W5$	33.5	$R11$	0.4
$L3$	10	$R1$	21.4	$R12$	0.75
$L4$	48.5	$R2$	20.9	$R13$	1.65
$L5$	0.66	$R3$	26.65	$R14$	1.5
$L6$	1.15	$R4$	0.6	$R15$	0.3
$L7$	39.5	$R5$	7.7	$R16$	0.75
$L8$	5.66	$R6$	17.5	$R17$	1.25
$W1$	55.5	$R7$	0.25	$H1$	2
$W2$	3.72	$R8$	2	$H2$	1
$W3$	1.2	$R9$	2.2	$H3$	5

3. ANTENNA DESIGN

The proposed double-layered stacked circularly polarized SIW cavity-backed antenna employs indirect stripline-to-SIW feeding transition, hereby exciting the circular patch radiator with proximity coupling method, thus effectively enhancing its bandwidth. To realize dual circular polarizations, a circular patch is excited by two pins, which are symmetrically located at the diagonal axis of the patch. And the two pins are excited by two separate 50-Ω striplines, which are connected to the four-port quadrature hybrid coupler made in stripline form. Then the quadrature hybrid coupler, based on 35-Ω and 50-$\Omega\lambda_{g0}/4$ transmission-line sections ($\lambda_{g0}/4$ refers to the dielectric wavelength at the center frequency of the CP band), provides input signal equal in amplitude and 90° out of phase needed for CP antenna to the dual linear modes of the circular radiator patch. RHCP is generated from input Port 1 with Port 2 terminated with a matched load, while LHCP is generated from input Port 2 with Port 1 terminated with a matched load. For fabrication convenience, the Q-hybrid stripline is enclosed with plated-through via holes from the top ground to bottom ground of the Q-hybrid substrate in practice, which form a cavity to suppress the excitation of the unwanted parallel-plate mode. Additionally, the proposed antenna is designed to be bottom-fed instead of side-fed, which facilitates eliminating two SMA connectors' interfering with the radiated field.

The methods of enhancing the antenna bandwidth are interpreted as follows. First, as illustrated in Figure 2(a) (the surface current with red color refers to the dominant surface current), the surface currents are mainly distributed on the circular patch, while relatively stronger parasitic coupling resonant currents also exist on the surface area enclosed by the SIW cavity and the annular slot. The surface current distribution balance shown in Figure 2(a) indicates that multiple resonances of

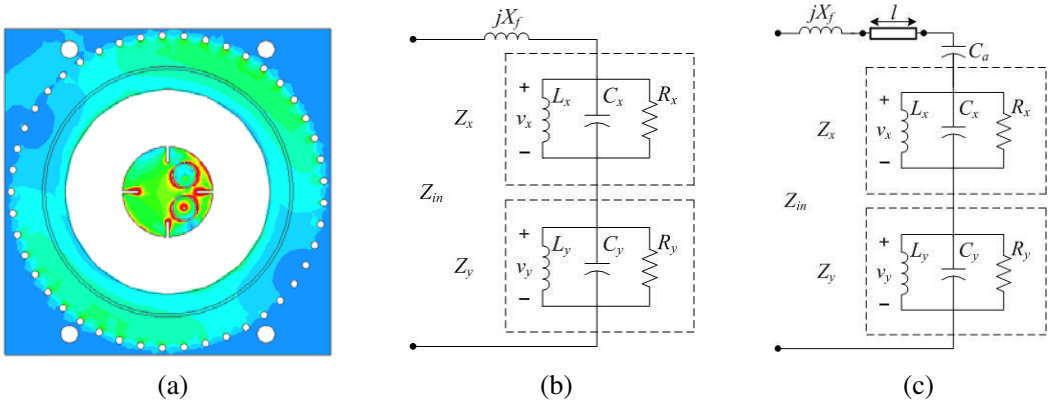

Figure 2. Current distribution and circuit models. (a) surface current distribution of the proposed antenna's top metal layer; (b) circuit model of the conventional single-fed circular patch antenna; (c) circuit model of the improved single-fed circular patch antenna loaded with a ring slot.

dual linear polarization modes can be generated by the circular patch radiator, SIW cavity resonator, and annular slot resonator together. With discreetly tuning their dimensions to make these resonances properly close to each other, the antenna bandwidth will be effectively broadened. Second, two ring slots are loaded around the circular patch radiator's two feeding points. Figures 2(b) and (c) provide the equivalent circuit models of a conventional circular patch antenna and an improved circular patch antenna loaded with a ring slot, respectively. For ease of the qualitative analysis, they are both assumed single-fed. In the dual-parallel RLC circuit models, X_f represents the probe inductance, while Z_x and Z_y represent the RLC circuit models corresponding to the patch antenna's two modes which radiate x-polarized and y-polarized waves towards broadside, respectively. In Figure 2(c), the ring slot introduces a radial capacitance denoted as C_a. Meanwhile, an additional transmission line with length of l is introduced to model the effect of the radial parallel plate transmission line (RPPTL). Since the radius of the ring slot is much smaller than the substrate thickness, the effect of the RPPTL can be negligible. And the ring slot results in merely a simple capacitor compensating for the probe reactance. Thus, each inserted ring slot can be seen as a capacitive element in series with its corresponding probe's inductance, thereby removing the probe reactance [12]. The AR bandwidth can be significantly enhanced with the presence of the two ring slots. Third, four rectangular slots are symmetrically loaded on the circular patch radiator, which provide a longer pathway for the surface current of the excited circular patch, thus lowering the antenna resonant frequency and equivalently miniaturizing the antenna size. Finally, a parasitic ring slot is etched on the upper metal layer of the SIW cavity acting as a perturbation

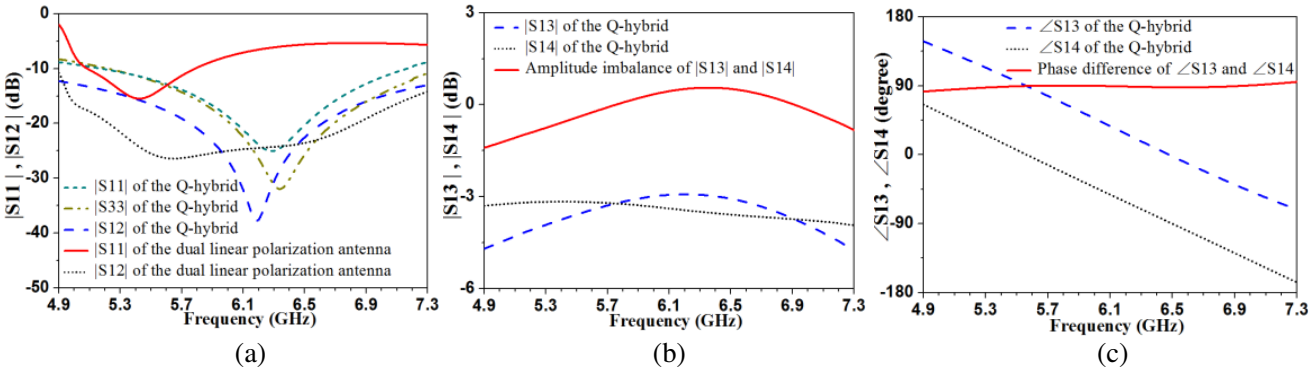

Figure 3. Simulated S-parameters of the SIW cavity-backed dual linear polarization antenna and Q-hybrid. (a) $|S11|$ and $|S12|$ of the dual-polarized antenna and Q-hybrid; (b) amplitude imbalance between the Q-hybrid's output ports; (c) phase difference between the Q-hybrid's output ports.

structure to further adjust and improve the AR performance.

Figure 3 provides the simulated S-parameter performance of the single SIW cavity-backed dual linear polarization antenna and the single Q-hybrid (port 1: input port, port 2: isolated port, port 3: through port, port 4: coupled port) separately. Figure 3(a) reveals that the impedance bandwidths ($|S11| \leq -10$ dB) of the single dual-polarized antenna and the single Q-hybrid are 14.0% (5.06–5.82 GHz) and 33.2% (5.15–7.2 GHz), respectively. Meanwhile, across the bandwidth of 5.15–7.2 GHz, $|S12|$ of the dual-polarized antenna's two input ports is less than -15.2 dB, while $|S12|$ of the Q-hybrid's two input ports is less than -13.6 dB. In Figures 3(b) and (c), the amplitude imbalance between the Q-hybrid's two output ports is less than 1.0 dB, and their phase difference is approximately maintained at 90° (86.0°–93.4°) within 5.15–7.2 GHz. Actually, during the process of antenna optimization design, it can be observed that the Q-hybrid mainly accounts for the proposed antenna's wide impedance bandwidth, while the introduction of the two ring slots on the circular patch radiator significantly improves its AR bandwidth. Besides, the proposed antenna's low-profile characteristic mainly results from its inherent SIW cavity-backed structure.

4. SIMULATED AND MEASURED RESULTS

In order to facilitate the manufacture, the proposed dual circularly polarized SIW cavity-backed antenna with the parameters shown in Figure 1 is fabricated and measured. The measured and simulated VSWRs of the proposed antenna are depicted in Figure 4. With reference to the figure, the simulated and measured impedance bandwidths (VSWR $\leq$ 2) of the proposed antenna for Port 1 (RHCP) are 46.0% (4.77–7.62 GHz) and 45.7% (4.74–7.55 GHz), respectively, while 46.0% (4.77–7.62 GHz) and 46.2% (4.75–7.6 GHz) for Port 2 (LHCP), respectively.

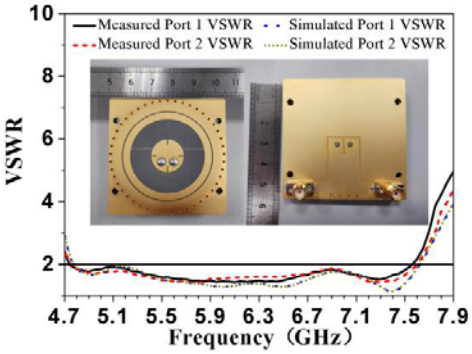

Figure 4. Simulated and measured VSWRs and the photographs of the fabricated antenna.

Figure 5 shows the simulated and measured normalized radiation patterns in the XZ-plane and YZ-plane at 5.2, 5.8 and 6.4 GHz. In Figure 6, the measured RHCP gains are from 4.8 dBic to 7.6 dBic with an average RHCP gain of 6.4 dBic, while the measured LHCP gains are from 4.9 dBic to 7.5 dBic with an average LHCP gain of 6.3 dBic. From Figure 5 and Figure 6, it can be seen that relatively stable pattern characteristics are obtained. Meanwhile, the simulated and measured 3-dB AR bandwidths (AR $\leq$ 3) for RHCP (Port 1) are 36.8% (4.77–6.92 GHz) and 37.5% (4.74–6.93 GHz), respectively, while the simulated and measured 3-dB AR bandwidths (AR $\leq$ 3) for LHCP (Port 2) are 36.8% (4.77–6.92 GHz) and 37.2% (4.75–6.92 GHz), respectively. It should be noted that the discrepancy between the simulated and measured results may be caused by the imperfect testing environment, which is mainly due to the interferences from indoor reflection. Furthermore, the errors in the process of fabrication, namely the errors resulting from limited processing accuracy and errors of non-uniformity of the substrate with respect to relative dielectric constant and loss tangent, and the non-ideality in welding may be taken into account as well. In addition, the measured effective dual CP bandwidth of 37.2% (4.75–6.92 GHz) not only includes certain Wi-Fi (5.2/5.8 GHz) or WiMAX (5.5 GHz) band communication application, but also offers the potential to implement multiservice transmission.

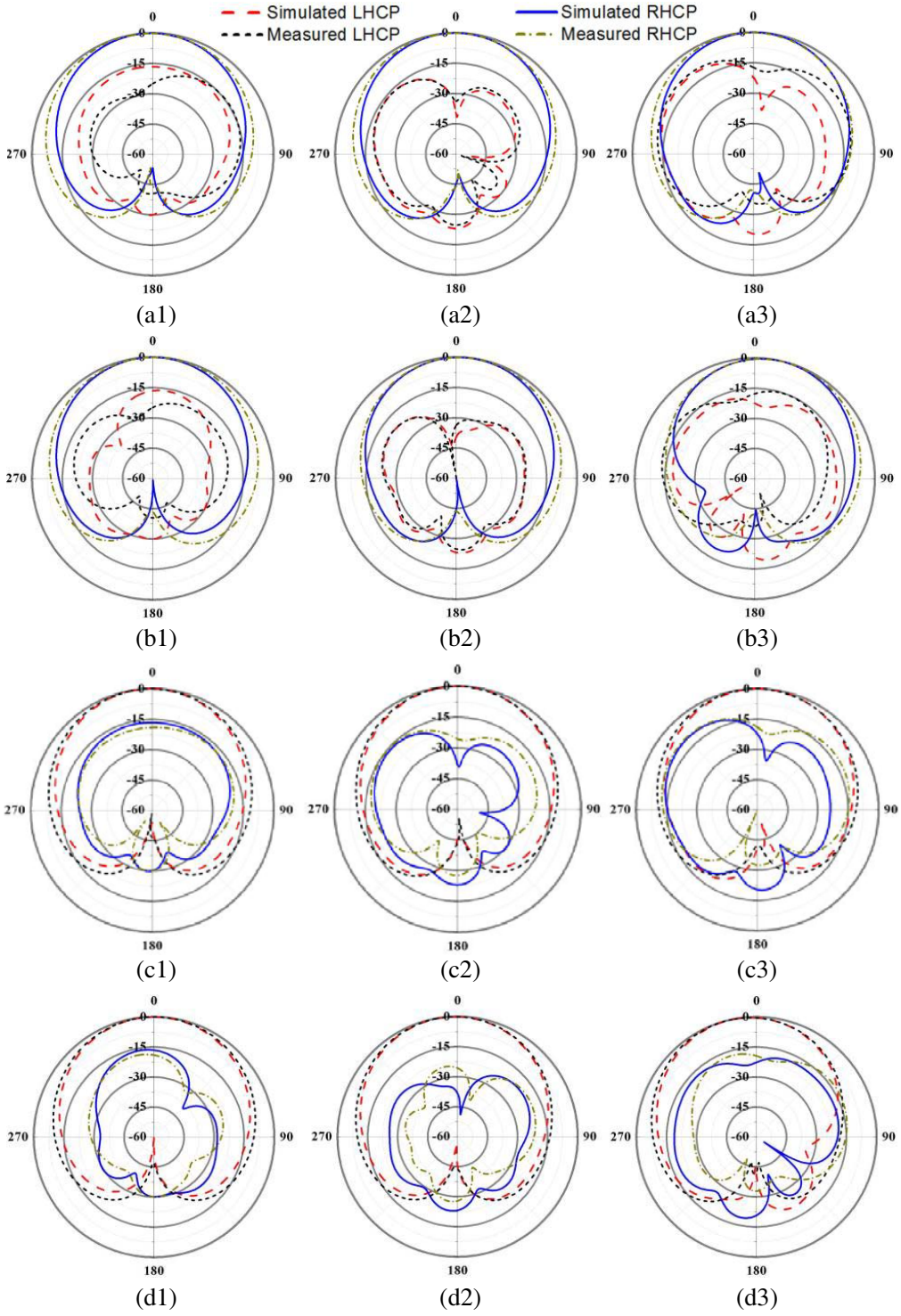

Figure 5. Simulated and measured radiation patterns. When Port 1 is excited: (a1) XZ-plane at 5.2 GHz; (a2) XZ-plane at 5.8 GHz; (a3) XZ-plane at 6.4 GHz; (b1) YZ-plane at 5.2 GHz; (b2) YZ-plane at 5.8 GHz; (b3) YZ-plane at 6.4 GHz. When Port 2 is excited: (c1) XZ-plane at 5.2 GHz; (c2) XZ-plane at 5.8 GHz; (c3) XZ-plane at 6.4 GHz; (d1) YZ-plane at 5.2 GHz; (d2) YZ-plane at 5.8 GHz; (d3) YZ-plane at 6.4 GHz.

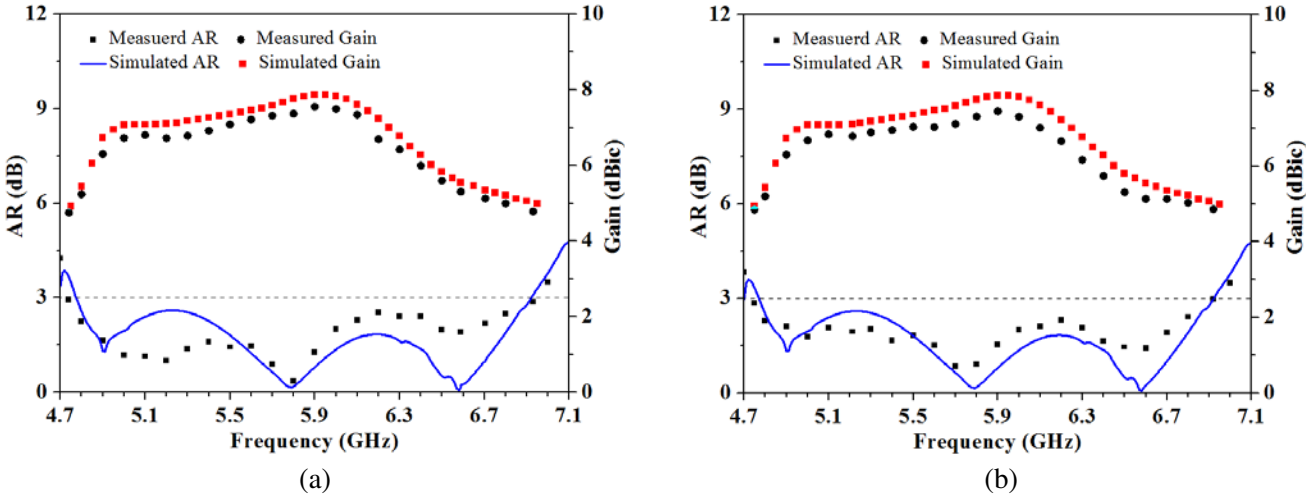

Figure 6. Simulated and measured ARs and gains of the proposed antenna when (a) Port 1 is excited and (b) Port 2 is excited.

Table 2. Comparison with other referenced antennas. (BW: Effective dual-CP/RHCP bandwidths).

Reference Designs	BW (GHz)	Substrate ε_r	Antenna Height (mm)	Peak Gain (dBic)
Proposed Antenna	4.75–6.92 (37.2%)	2.65/2.94	5 ($0.097\lambda_0$)	7.6 dBic at 5.9 GHz
Kumar et al. [4]	11.8–13.2 (11.2%)	2.2	0.787 ($0.03\lambda_0$)	4.7 dBic
Yang et al. [5]	4.77–5.39 (12.4%)	2.2/4.4	4.112 ($0.069\lambda_0$)	7.1 dBic at 5.2 GHz
Zhu et al. [6]	54.2–64.3 (17.2%)	2.2	0.787 ($0.16\lambda_0$)	13.7 dBic
Kumar et al. [7]	3.4% around 9.3 GHz	2.2	2.4 ($0.07\lambda_0$)	5.7 dBic
Mao et al. [8]	19.4% around 5.4 GHz	2.2/3.55	5.054 ($0.091\lambda_0$)	7.9 dBic at 5.3 GHz
Cai et al. [9]	17.6–19.8 (11.8%)	2.2	4.3 ($0.27\lambda_0$)	10.3 dBic
Luo et al. [10]	18–20.5 (13.0%)	2.2/1.04/3.55	3.654($0.23\lambda_0$)	about 4.9 dBic
Yang et al. [11]	4.8–7.4 (43.3%)	4.4/2.55	15 ($0.3\lambda_0$)	8.6 dBic at 7.4 GHz

A comparison of the proposed antenna with published referenced work is made in terms of effective dual-CP/RHCP bandwidth, relative dielectric constant of the substrate, antenna height, and peak gain with results presented in Table 2. The selected criteria for inclusion in this comparison are newly published unidirectional dual-CP/RHCP antennas. Compared with the dual-CP antennas presented in [4–10], the proposed antenna obtains a much wider effective dual CP bandwidth, without sacrificing the antenna profile performance significantly. Meanwhile, though the RHCP antenna presented in [11] has an advantage on the proposed antenna in effective CP bandwidth, its antenna profile is much higher than that of the proposed antenna. Consequently, from Table 1, it can be seen that the proposed antenna provides either a wider effective dual CP bandwidth or a lower profile. Actually, it obtains a better performance with a favorable compromise between operating bandwidth and antenna profile.

5. PARAMETRIC STUDY

All critical physical parameters, such as $R5$, $R9$, $R3$, $R6$, $W4$, and $H3$, should be adjusted carefully to achieve a good performance. In this section, the effects of these parameters on impedance and AR bandwidths are examined in detail to facilitate the design of a same or homogeneous antenna with different specifications. During this process, all the other parameters not mentioned stay constant as shown in Table 1. Additionally, considering the proposed dual CP antenna's completely symmetric

structure with reference to X-axis resulting in the symmetry of the dual CP radiation, this section only shows the simulation results when Port 1 is excited.

5.1. Effect of Circular Patch Radiator (R5 and R9)

The effects of the circular patch radiator ($R5$ and $R9$) on the impedance and AR bandwidths are shown in Figure 7 and Figure 8, respectively. As expected, as $R5$ increases, the whole operating band shifts toward lower band. Meanwhile, when two ring slots are introduced with discreetly optimized widths of 0.2 mm, the antenna performance both in impedance and AR bandwidths can be greatly enhanced, especially for the AR performance at the lower frequencies. To obtain good impedance matching and AR performance, $R5$ and $R9$ are set as 7.7 mm and 2.2 mm, respectively.

5.2. Effect of SIW Cavity and Annular Slot (R3 and R6)

Figure 9 and Figure 10 reveal the influence of the SIW cavity ($R3$) and the annular slot ($R6$) on the impedance and AR bandwidths, respectively. As $R3$ increases, the impedance and AR bandwidths at lower band will be broadened. Meanwhile, compared to the impedance performance, the AR

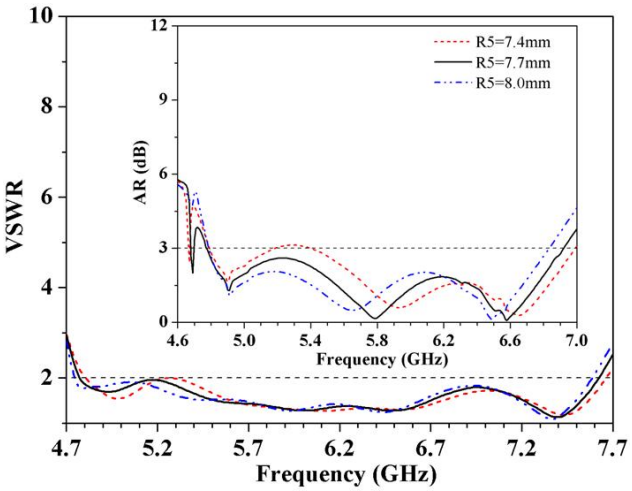

Figure 7. VSWRs and ARs with varied $R5$.

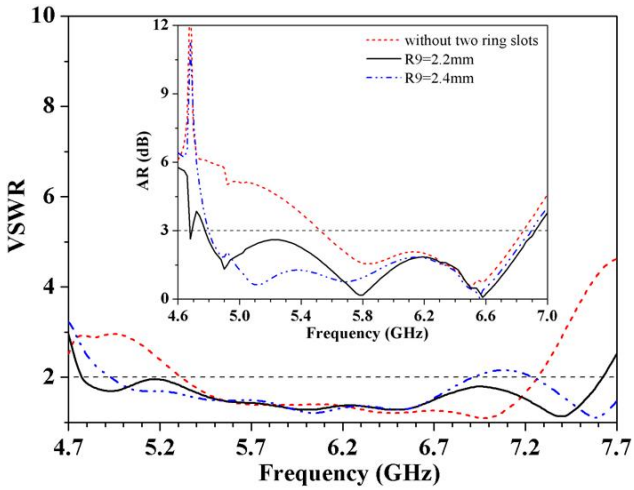

Figure 8. VSWRs and ARs with varied $R9$.

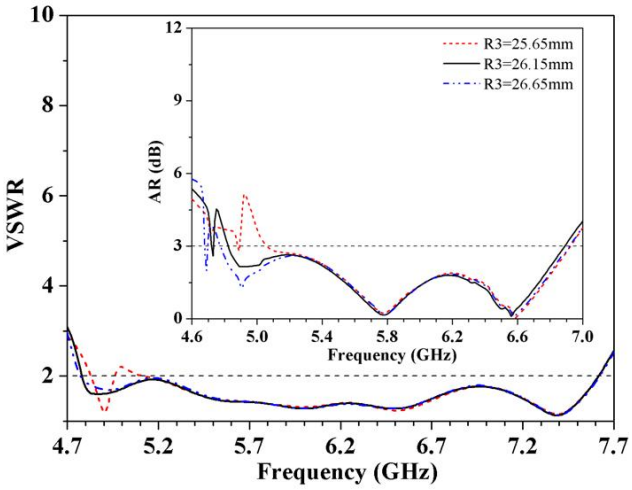

Figure 9. VSWRs and ARs with varied $R3$.

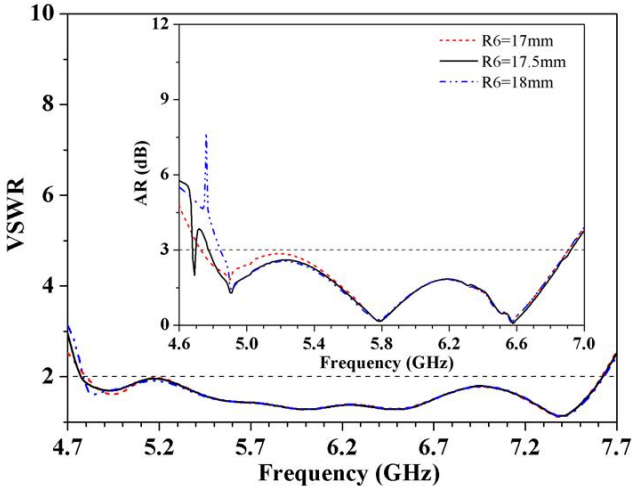

Figure 10. VSWRs and ARs with varied $R6$.

performance is much more sensitive to varied $R3$. Moreover, as $R6$ increases, the AR performance at lower frequencies will degrade, while the AR performance at middle and higher frequencies almost stays the same. However, the impedance bandwidth will degrade, whether the values of $R6$ increases or decreases. To obtain a wider effective CP bandwidth, $R3$ and $R6$ are optimized as 26.65 mm and 17.5 mm, respectively.

5.3. Effect of Ring Slot, Quadrature Hybrid Coupler and Antenna Height (W4 and H3)

The effects of the quadrature hybrid coupler ($W4$) and antenna height ($H3$) on the impedance and AR bandwidths are shown in Figure 11 and Figure 12, respectively. As $W4$ increases, the impedance bandwidth shifts toward lower band. However, the AR bandwidth is very sensitive to varied $W4$, especially for lower frequencies. Meanwhile, both the impedance and AR bandwidths are very sensitive to the antenna height $H3$. To obtain good impedance matching and AR performance, $W4$ and $H3$ are carefully tuned as 7.7 mm and 5 mm, respectively.

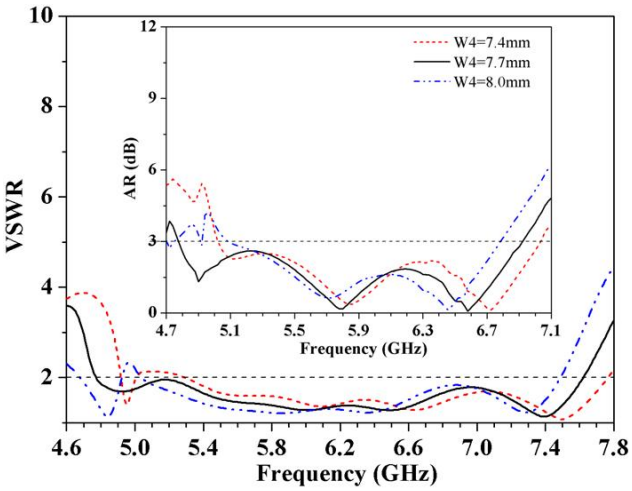

Figure 11. VSWRs and ARs with varied $W4$.

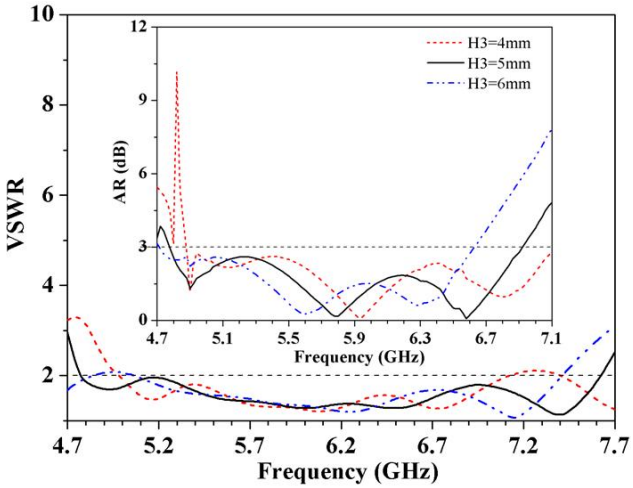

Figure 12. VSWRs and ARs with varied $H3$.

6. CONCLUSION

A dual-CP SIW cavity-backed antenna with enhanced bandwidth and reduced size has been presented. Simulation and measurement results indicate that with the improved SIW cavity and radiator patch, it can produce an effective dual CP bandwidth of 37.2% (4.75–6.92 GHz). The effects of all critical parameters on impedance and AR bandwidths are studied in detail to facilitate the design of a same or homogeneous antenna. Meanwhile, relatively moderate RHCP gains, from 4.8 dBic to 7.6 dBic with an average gain of 6.4 dBic, and relatively stable LHCP gains, from 4.9 dBic to 7.5 dBic with an average gain of 6.3 dBic, are yielded simultaneously. With these inherent characteristics, the proposed antenna can be a good candidate for wideband wireless applications.

REFERENCES

1. Li, J.-F., D.-L. Wu, G. Zhang, Y.-J. Wu, and C.-X. Mao, "A left/right-handed dual circularly-polarized antenna with duplexing and filtering performance," *IEEE Access*, Vol. 7, 35431–35437, Apr. 2019.
2. Yang, Y.-H., B.-H. Sun, and J.-L. Guo, "A low cost, single-layer, dual circularly polarized antenna for millimeter-wave applications," *IEEE Antennas Wireless Propag. Lett.*, Vol. 18, No. 4, 651–655, 2019.

3. Ferreira, R., J. Joubert, and J.-W. Odendaal, "A compact dual-circularly polarized cavity-backed ring-slot antenna," *IEEE Trans. Antennas Propag.*, Vol. 65, No. 1, 364–368, Jan. 2017.
4. Kumar, A. and S. Raghavan, "Broadband dual-circularly polarised SIW cavity antenna using a stacked structure," *Electron. Lett.*, Vol. 53, No. 17, 1171–1172, Aug. 2017.
5. Yang, W.-C., Q. Meng, W.-Q. Che, L.-Z. Gu, and Q. Xue, "Low-profile wideband dual-circularly polarized metasurface antenna array with large beamwidth," *IEEE Antennas Wireless Propag. Lett.*, Vol. 17, No. 9, 1613–1616, Sep. 2018.
6. Zhu, J.-F., S.-W. Liao, Y. Yang, S.-F. Li, and Q. Xue, "60 GHz dual-circularly polarized planar aperture antenna and array," *IEEE Trans. Antennas Propag.*, Vol. 66, No. 2, 1014–1019, Feb. 2018.
7. Kumar, K., S. Dwari, and M.-K. Mandal, "Broadband dual circularly polarized substrate integrated waveguide antenna," *IEEE Antennas Wireless Propag. Lett.*, Vol. 16, 2971–2974, Nov. 2017.
8. Mao, C.-X., S. Gao, Y. Wang. and J.-T.-S. Sumantyo, "Compact broadband dual-sense circularly polarized microstrip antenna/array with enhanced isolation," *IEEE Trans. Antennas Propag.*, Vol. 65, No. 12, 7073–7082, Dec. 2017.
9. Cai, Y., Y.-S. Zhang, Z.-P. Qian, W.-Q. Cao, and S.-J. Shi, "Compact wideband dual circularly polarized substrate integrated waveguide horn antenna," *IEEE Trans. Antennas Propag.*, Vol. 64, No. 7, 3184–3188, Feb. 2016.
10. Luo, Q., S. Gao, and L. Zhang, "Wideband multilayer dual circularly polarised antenna for array application," *Electron. Lett.*, Vol. 51, No. 25, 2087–2089, Dec. 2015.
11. Yang, W.-W. and J.-Y. Zhou, "Wideband circularly polarized cavity-backed aperture antenna with a parasitic square patch," *IEEE Antennas Wireless Propag. Lett.*, Vol. 13, 197–200, Feb. 2014.
12. Kovitz, J.-M. and Y. Rahmat-Sammi, "Using thick substrates and capacitive probe compensation to enhance the bandwidth of traditional CP patch antennas," *IEEE Trans. Antennas Propag.*, Vol. 62, No. 10, 4970–4979, Oct. 2014.